Draft version November 15, 2021
Typeset using LaTeX default style in AASTeX631

Direct observation of the radial magnetic field gradient in HD 58260 from spectropolarimetry of NLTE lines in emission

Marina Giarrusso [1]

[1] *INFN - Laboratori Nazionali del Sud, Via S. Sofia 62, I–95123 Catania, Italy*

Submitted to ApJ

ABSTRACT

Because of the unquestionable presence of magnetic fields in stars, their role in the structure of stellar atmospheres has for a long time been a subject of speculation. In our contribution to this discussion we present spectropolarimetric evidence of the decrease of the radial component of the magnetic field with altitude in the atmosphere of HD 58260, a B-type magnetic star on the main sequence. We show that the Stokes V profiles of metal lines in emission of the outer atmosphere are evidence for a field three times weaker than from absorption lines from inner layers. The extra flow of energetic particles due to the magnetic-gradient pumping mechanism could be at the origin of the magnetospheres surrounding this class of stars and at the basis of the high energy phenomena observed. We also list a series of spectral lines useful for measuring the surface field of early-type stars.

Keywords: Plasma astrophysics – Spectropolarimetry – Atomic spectroscopy – Spectral line identification – Spectral line list – Magnetic Fields – Magnetic Stars – Stars: individual: HD 58260

1. INTRODUCTION

The understanding of astrophysical plasmas has improved after the inclusion of magnetic field effects in radiative transfer and polarization (Landi Degl'Innocenti & Landolfi 2004). The introduction of magnetic fields to the modeling of atomic diffusion (Alecian & Stift 2019) also has provided precious insight into the buildup of abundance anomalies. On the other hand, little has been done to take into account the contribution of magnetic fields to the various equilibria in stellar atmospheres. Only semi-quantitative approaches have been proposed, with sometimes surprising conclusions. For example, Hubbard & Dearborn (1982) have claimed that the radii of magnetic Ap stars are 20% larger than those of main sequence stars with the same temperature, a result that would challenge our current view of the atmospheres of magnetic stars.

This paucity of efforts is a consequence of the lack of observational evidence of a radial gradient in the field strength that is necessary to give rise to a magnetic pressure. Wolff (1978) made the first-ever attempt to derive the magnetic gradient in stellar atmospheres by measuring the longitudinal component of the field from lines formed from optical depth $\log \tau_{500\,\mathrm{nm}} = 0.42$ to 0.03. It was found that variations, if present at all, are not larger than 20%. In similar studies, Nesvacil et al. (2004); Romanyuk & Kudryavtsev (2004); Kudryavtsev & Romanyuk (2009) have reported magnetic fields $5 - 25\%$ stronger in the inner layers (where spectral lines shortward of the Balmer jump are formed) with respect to the outermost layers (where spectral lines longwards of the Balmer jump come from). The investigation by Wolff (1978) was hampered by the modest depth of the visible stellar disk $T_{\mathrm{eff}} \sim 8000\,\mathrm{K}$ atmospheres examined ($\log \tau_{500\,\mathrm{nm}}$ changes from 1 to -3 over just 1600 km).

Early B-type stars are more suitable objects to look for a field gradient; their outer layers turn "visible" when metal spectral lines are in emission. Sigut et al. (2000) reported for the first time the presence of metal lines in emission in

marina.giarrusso@lns.infn.it

Table 1. Atomic transitions – resulting in a Zeeman doublet with two π components in coincidence with two σ components – suitable for measuring the surface magnetic field of B-type stars. Line-by-line B_s measurements are from a double Gaussian function fit to the two components (see Figure 1).

Ion	Å	Configuration	Term	J	g_L	Configuration	Term	J	g_L	B_s (G)
C II	6787.207	$2s^2 2p^2\,(^3P^o)\,3s$	$^4P^o$	1/2	2.67	$2s^2 2p^2\,(^3P^o)\,3p$	^4D	1/2	0.00	4200±140
Si II	6699.401	$3s\ 3s^3\,(^3P^o)\,4s$	$^4P^o$	1/2	2.67	$3s\,3p^2\,(^3P^o)\,4p$	^4D	1/2	0.00	4320±130
S II	4278.516	$3s^2 3p^2\,(^3P)\,4p$	$^4P^o$	1/2	2.67	$3s^2 3p^2\,(^3P)\,4d$	$^4D^o$	1/2	0.00	4700±160
S II	4456.382	$3s\ 3s^2\,(^3P)\,4p$	$^4D^o$	1/2	0.00	$3s^2 3p^2\,(^3P)\,5s$	^4P	1/2	2.67	4400±270
S II	5473.614	$3s^2 3p^2\,(^3P)\,4s$	^4P	1/2	2.67	$3s^2 3p^2\,(^3P)\,4p$	$^4D^o$	1/2	0.00	4440±40

the visible spectrum of B-type stars. These authors suggested that in this class of stars emission lines are produced by Non-Local Thermodynamic Equilibrium (NLTE) effects because of source functions rising with the atmosphere height without the necessity of a temperature inversion (chromosphere). A conclusion theoretically supported by Alexeeva et al. (2016, 2018, 2019); Mashonkina (2020); Mashonkina et al. (2020). From an analysis of line profiles of a sample of early B-type stars, Sadakane & Nishimura (2017) concluded that emission and absorption lines are equally broadened by the stellar rotation, supplying an observational proof that emission lines are from the outer stellar atmosphere and not from a circumstellar environment.

The present paper reports the results of a search for a radial gradient in the magnetic field of the early B-type star HD 58260, based on high-resolution Stokes I and V profiles of spectral lines in absorption and in emission, sampling at least 6 dex in optical depth. This magnetic (Bohlender et al. 1987) helium-rich (Garrison et al. 1977) star has been selected because of its very low projected rotational velocity ($v_{\rm eq} \sin i = 3$ km s^{-1}) and absence of evidence for either magnetic or light variability (Shultz et al. 2018, 2019a). All these properties simplify the procedure of measuring the magnetic field from spectral lines and the interpretation of results.

2. THE MAGNETIC FIELD OF HD 58260

Hereafter, definitions and measuring procedures of stellar magnetic fields are as in Leone et al. (2017). We just recall: 1) the effective – or longitudinal – magnetic field ($B_{\rm eff}$) is the average across the visible stellar disk of the longitudinal component of the field and 2) the surface magnetic field (B_s) is the average across the visible stellar disk of the field modulus.

2.1. *Effective Magnetic Field and Variability Period*

Shultz et al. (2018) measured the effective magnetic field of HD 58260 from ten high-resolution spectra in circularly polarized light collected with ESPaDOnS (R = $\lambda/\Delta\lambda$ = 68 000, Donati et al. 2006; Wade et al. 2016), between MJD = 56623 and 56678. With the inclusion of literature data, these authors conclude that this helium-rich star presents a $B_{\rm eff} = 1820 \pm 30$ G over a time-scale of $\sim$35 years, a lack of variability corroborated by the *Hipparcos* photometry. Within the framework of the Oblique Rotator Model (Babcock 1949), the constant magnetic field and the shape of the Stokes V profiles are due to the coincidence of the stellar rotational axis with the line-of-sight (LoS) (Shultz et al. 2019a).

From a further HARPS (R = 115 000, Mayor et al. 2003) spectrum in circularly polarized light (MJD = 57091.1462), Järvinen et al. (2018) measured $B_{\rm eff} = 1537 \pm 37$ G and classified HD 58260 as a magnetic variable. Even though this is possible, we note that both Shultz et al. (2018) and Järvinen et al. (2018) measured $B_{\rm eff}$ from the "average" least-squares deconvolution profile (Donati et al. 1997) under the assumption that Stokes V is the first derivative of Stokes I, and neglecting the fact that the line profiles of HD 58260 are shaped not only by the magnetic field but also by stellar rotation and instrumental broadening. Scalia et al. (2017) and Ramírez Vélez (2020) have performed numerical simulations to check the importance of these extra broadening mechanisms when measuring stellar magnetic fields. Here it is appropriate to quote one of Scalia et al. (2017) results: a $B_{\rm eff} = 3175$ G field would appear as 2495 G at R

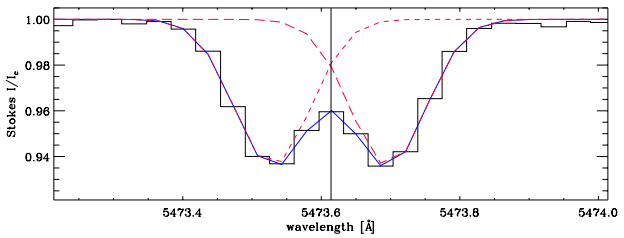

Figure 1. Histogram of the observed SII 5473.614 Å line. This splits in just two Zeeman subcomponents fitted with a double Gaussian function (blue-solid). In this case the distance between the two (red-dashed) components corresponds to $B_s = 4440 \pm 40$ G, as listed in Table 1.

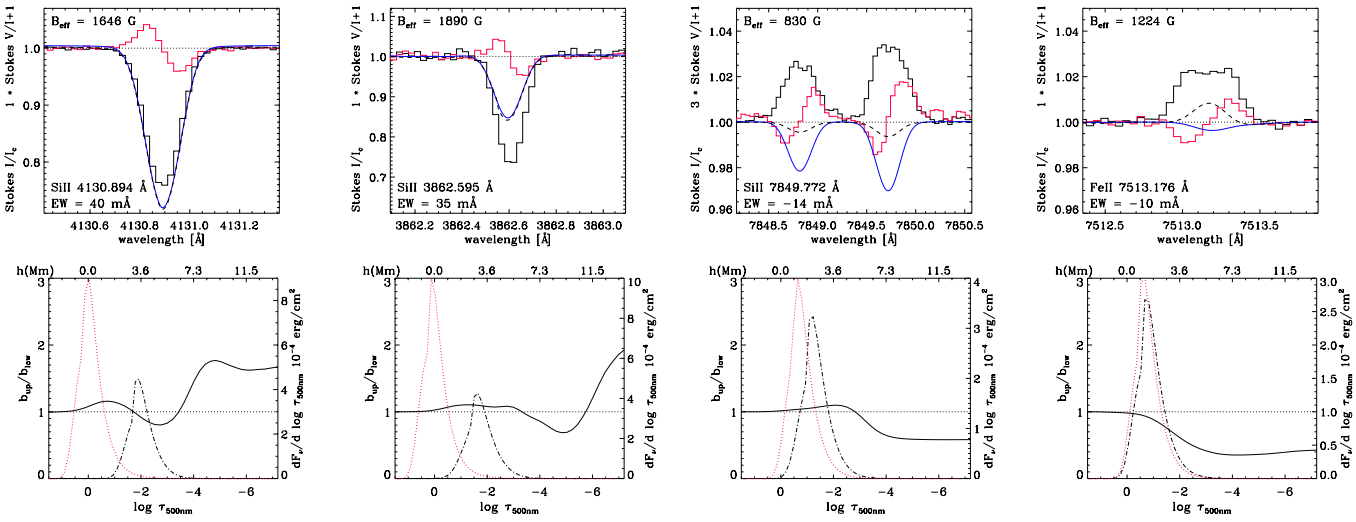

(a) (b) (c) (d)

Figure 2. Top: examples of Stokes I/I_c and V/I observed profiles (offset by unity), displayed as black and red histograms respectively, of lines in absorption (a, b) and emission (c, d). LTE (full) and NLTE (dashed) synthetic profiles are also reported. Bottom: Gray (1992) contribution function for both the line core (black dash-dotted) and the line continuum (red dotted), and ratio b_{up}/b_{low} between the departure coefficients of the involved levels (black solid), as a function of optical depth and geometrical height h. See Section 3 for details.

= 65 000 and an instrumental profile with FWHM = 2.5 pixels, equal to 1697 G with R = 115 000 and FWHM = 4 pixels. In addition, Shultz et al. (2018) and Järvinen et al. (2018) could give discrepant results because of different line lists differently sampling the non homogeneous distribution of elements on the surface of HD 58260. It is thus possible that the differences between ESPaDOnS and HARPS results are not conclusive and so the variable nature of HD 58260 remains to be confirmed.

Hereafter, we refer to the average Stokes I and V spectra of HD 58260 computed from the observations presented by Shultz et al. (2018). The Signal-to-Noise ratio is of the order of 1000 in the Stokes V continuum.

2.2. *The Surface Magnetic Field*

Following Mathys (1990), there is agreement that B_s is best measured using FeII 6149.258 Å, a spectral line representing a simple doublet arising from coinciding π and σ subcomponents. Since this line is absent from the spectra of early type stars, we have mined from the NIST five spectral lines present in the spectrum of HD 58260 that exhibit equally lucky quantum numbers to result in Zeeman doublets (Table 1). Fitting the observed doublets with double Gaussian functions (as shown in Figure 1 for SII 5473.614 Å line) we have obtained the B_s values listed in Table 1. The weighted average gives a surface field of HD 58260 equal to $B_s = 4430 \pm 40$ G.

2.3. *Magnetic Field Geometry*

As to a dipole with polar strength $B_{\rm p}$, Preston (1969) has shown:
1) for a LoS coincident with the dipole axis

$$B_{\rm s} = 0.68\frac{3.42-u}{3-u}B_{\rm p} \quad \text{and} \quad B_{\rm eff} = \frac{1}{20}\frac{15+u}{3-u}B_{\rm p} \tag{1}$$

2) when the LoS lies in the magnetic equatorial plane

$$B_{\rm s} = 0.68\frac{2.76-u}{3-u}B_{\rm p} \quad \text{and} \quad B_{\rm eff} = 0 \tag{2}$$

Here, u is the linear limb-darkening coefficient.

If the magnetic field of HD 58260 is dipolar and the LoS coincident with the rotation axis (Shultz et al. 2018), the ratio $B_{\rm eff}/B_{\rm s} = 1860/4430 \sim 0.42 \pm 0.06$ – which is close to the highest possible value of 0.37 ($u = 0.4$, Neiner et al. 2003) – also implying the coincidence of dipole and rotation axes and a polar field $B_{\rm p} \sim 6000$ G (consistent with the geometry and surface field strength determined by Shultz et al. (2019a)). See Section 3 for the adopted $B_{\rm eff}$ value.

3. $B_{\rm EFF}$ FROM EMISSION LINES

We selected the magnetic early B-type star HD 58260 for the presence of visible metal lines in emission, unquestionably with circularly polarized profiles (Figure 2). Keep in mind that Stokes V profiles of emission lines are reversed in sign with respect to absorption lines. Wade et al. (2012) already reported on the presence of not null Stokes V profiles in emission in the spectrum of the O7f?cp star NGC 1624-2. These authors also found a Stokes V change in sign between absorption and weak-emission OIII lines and propose to locate the formation region of these emission lines in the magnetosphere.

We ran the TLUSTY205 and SYNSPEC5.1 codes (Lanz & Hubeny 2007) to model – under the assumption of both LTE and NLTE – the spectral lines of HD 58260 for $T_{\rm eff} = 19000$ K, $\log g = 4.0$ (Sigut et al. 2000) and solar abundances. No attempt has been made to determine the stellar parameters by matching the line strengths. Computations were aimed at line identification and evaluation of departure coefficients. Figure 2 shows examples of observed spectral lines both in absorption and emission together with: *i)* the theoretical spectra computed in LTE and in NLTE, *ii)* the Gray (1992) contribution functions (which give the relative contribution of the different atmospheric layers) in the line center and in the corresponding continuum – computed in LTE – plotted vs. the optical depth at $\tau_{500\,\rm nm}$ (and the geometrical height), and *iii)* the ratio $b_{\rm up}/b_{\rm low}$ between the departure coefficients of the levels involved in the transition, where $b = n_{\rm NLTE}/n_{\rm LTE}$ (being $n_{\rm NLTE}$ and $n_{\rm LTE}$ the actual population and the LTE population of a level, respectively). With a value < 1, lines in emission have an NLTE origin in the outer atmospheric layers of HD 58260.

We measured $B_{\rm eff}$ line by line both from absorption and emission profiles, using the first order momentum of Stokes V (Mathys 1994). From 16 lines in emission (Table 2) we obtained an average value of $B_{\rm eff} = 675 \pm 260$ G. The average from 84 absorption lines is $B_{\rm eff} = 1860 \pm 230$ G. Estimated from equation 15 by Mathys (1994), errors are $\propto EW^{-1}$ and dominated here by the very small equivalent widths of lines selected to sample the optical depth as widely as possible. To test the hypothesis that our sample of $B_{\rm eff}$ measurements from emission lines was drawn at random of the same population of $B_{\rm eff}$ measurements from absorption lines, the Student $t-$statistics has been applied. The significance of 2.7×10^{-33} indicates that the $B_{\rm eff}$ measurements from emission and absorption lines have different means. Also Wade et al. (2012) found $B_{\rm eff}$ from weak-emission lines about a factor 2 smaller than from absorption lines.

Locating the region of the formation of a line in emission depends on the adopted atmospheric model and the atomic parameters. Figure 2(c) shows the present limit of NLTE computations in the case of the two silicon lines in emission at 7849 Å. Theoretically, the population levels are significantly inverted locating the formation regions of these two lines at $\log \tau_{500\rm nm} < -4$ (bottom panel), but with SYNSPEC5.1 these lines are still in absorption (top panel). Even worse, not every line can at present be treated under the NLTE approximation. For a quantitative representation of NLTE effects on the 100 examined spectral lines with clearly observable Stokes V profiles we establish the relative difference between the observed equivalent width ($\rm EW_{Obs}$) and the expected value in the LTE approximation ($\rm EW_{LTE}$): $r = (\rm EW_{Obs} - EW_{LTE})/EW_{LTE}$. With LTE lines always in absorption, the zero value of the r-scale depends only on the observed lines and the scale can only be shrinked or expanded by assuming a different temperature or surface gravity of the LTE atmosphere. The idea behind this: the smaller r, the further out the line formation region. Figure 3

Table 2. Spectral lines in emission from which it was possible to measure the effective longitudinal field $B_{\rm eff}$ (in Gauss). Measured equivalent widths EW (in mÅ) and adopted effective Landé factors $g_{\rm eff}$ are also listed, together with the Chi-Square Probability Function p of the single-line measurements from the mean spectrum as in Donati et al. (1992): magnetic field detection (D) for $p > 0.99$, marginal detection (MD) for $0.95 < p < 0.99$, no detection (ND) for $p < 0.95$.

Ion	Å	EW	$g_{\rm eff}$	$B_{\rm eff}$	p
Si II	6239.665	−13.4	0.93	685±140	D
Si II	6818.414	−2.2	0.83	175±760	D
Si II	6829.799	−3.4	0.83	720±430	D
Si II	7848.816	−10.6	0.90	560±190	D
Si II	7849.722	−14.4	1.06	830±125	D
Fe II	4948.791	−0.6	1.14	650±870	ND
Fe II	5144.352	−1.2	0.89	745±700	ND
Fe II	5247.956	−1.8	0.73	620±825	D
Fe II	5251.226	−2.2	1.48	195±415	ND
Fe II	5429.987	−1.7	1.06	690±540	ND
Fe II	5493.831	−1.3	1.06	905±700	D
Fe II	5780.128	−1.4	1.00	415±955	D
Fe II	7513.176	−10.4	1.30	1225±200	D
Fe II	8490.102	−6.7	1.03	855±245	D
Fe II	8499.617	−4.3	0.89	815±235	MD
Fe II	8722.461	−4.5	1.10	730±330	D

visualizes the dichotomy between the $B_{\rm eff}$ values from the 84 absorption ($r > -1$) lines and the 16 emission ($r < -1$) lines respectively.

For lines in emission, inverted populations of the atomic levels at $\log \tau_{500\,\rm nm} < -4$ is corresponding to an altitude of tens of Mm above the layers with unit optical depth, where absorption lines are mainly formed (see Figure 2 showing their contribution functions). The scale of the vertical gradient of the magnetic field is $\sim 0.1\,{\rm G\,km^{-1}}$. This is a value much larger than what results for a magnetic dipole, for which it would be necessary to go to a distance of $0.4\,R_*(\sim 0.4\,\times 3R_\odot \approx 840\,{\rm Mm})$ from the surface of HD 58260 to experience a decrease of the field to 600 G from the surface value of 1800 G. An unrealistic extended atmosphere for the current view of magnetic early-type stars whose radii are not too different than for main-sequence stars with equal temperature (Shultz et al. 2019b).

Before drawing specific conclusions about the large difference between $B_{\rm eff}$ values from spectral lines in absorption (1860±230 G) and in emission (675±260 G), the importance of limb-darkening (see Section 2.3) has to be understood. From previous Preston (1969) relations (Eqs. 1), a *limb-brightening* for $u \sim -2.7$ could analytically reconcile this difference. A possibility ruled out by SYNSPEC5.1 intensities of spectral lines: limb-brightening (Figure 4) due to NLTE effects is not so large to justify the measured differences in the longitudinal field from lines in absorption and emission. Figure 4 also shows an almost constant brightness across the visible disk for lines in emission of a few mÅ eventually resulting in $B_{\rm eff} \sim 1550$ G. In conclusion, in the framework of present NLTE modeling of early B-type stars, the longitudinal component of the photospheric magnetic field of HD 58260 is decreasing with the stellar radius.

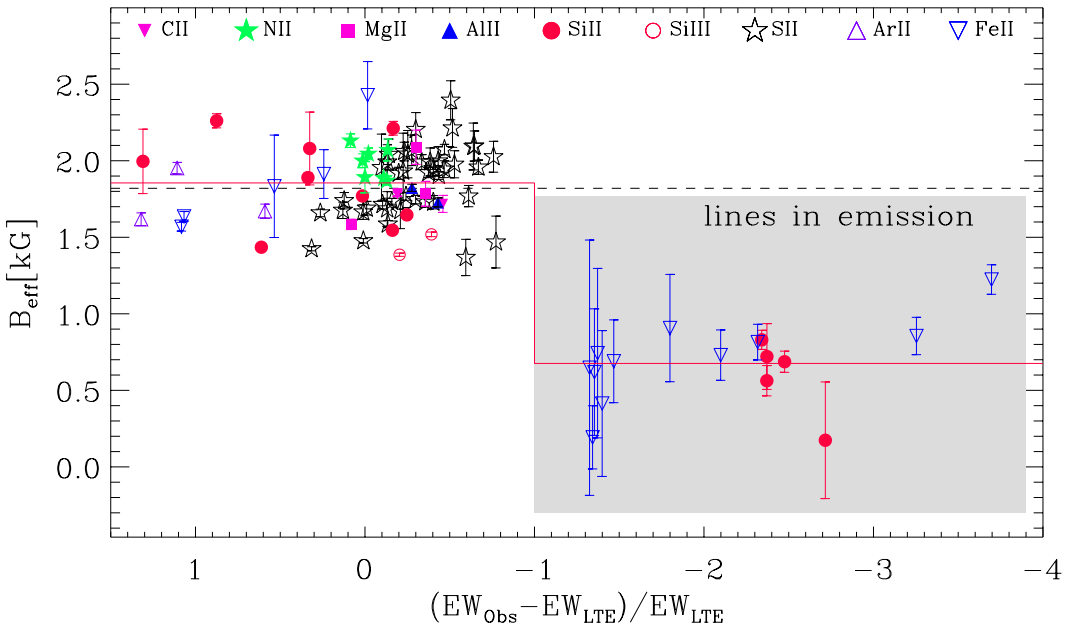

Figure 3. Line by line measurements of $B_{\rm eff}$ from nine different species vs. the relative differences between measured ($EW_{\rm Obs}$) and theoretical LTE ($EW_{\rm LTE}$) equivalent widths. The smaller the abscissa value, the further out the line formation region. The filled region contains lines in emission. The dashed line represents the field as measured by Shultz et al. (2018). The broken line goes through the average field values for absorption and emission spectral lines.

4. DISCUSSION AND CONCLUSIONS

We have measured the surface magnetic field of HD 58260 from newly identified spectral lines that split into a Zeeman doublet with the σ components in coincidence with the π components (see Table 1). These doublets are in general suitable for measuring the surface field of early type stars, as the FeII 6149.258 Å one is for cool magnetic stars. Obtained from spectral lines in absorption, the measured ratio $B_{\rm eff}/B_{\rm s}$ favors a coincidence of line-of-sight, rotation axis and dipole axis; the polar field value is of the order of 6000 G.

The metal emission lines of HD 58260 constitute extreme evidence for the breakdown of the LTE approximation in early type magnetic stars, but absorption lines are affected by NLTE too. Systematic differences in the optical depth between observed and LTE equivalent widths in magnetic stars, as a class, are commonly interpreted as due to a vertical stratification of elements (Catanzaro et al. 2016, 2020). Nevertheless, for these stars the attempt to reproduce observed metal emission lines by taking into account the NLTE effect works in the direction to smooth abundance gradients (Alexeeva et al. 2016, 2019; Mashonkina 2020; Mashonkina et al. 2020). Remaining differences between observed and theoretical lines could be a matter of present limits of NLTE modeling that needs to be improved for treating the upper atmospheric regions, or the consequence of level populations distorted by the far-UV (Wahlgren & Hubrig 2004) and/or X-ray (Mitskevich & Tsymbal 1992) radiation from the magnetosphere wrapping this class of stars (Shore & Brown 1990). HD 58260 appears an example of the necessity for a simultaneous and integrated study of atmosphere and magnetosphere.

HD 58260 presents emission lines with non-null Stokes V profiles. Determined via the first-order momentum of these profiles (Mathys 1994), the measured longitudinal magnetic field from these lines ($\sim$675 G) is three times weaker than from lines in absorption ($\sim$1860 G). Following Sadakane & Nishimura (2017), we conclude that emission lines originate from the outermost layers and that the magnetic field decreases with altitude in the atmosphere more fastly than expected for a dipolar field. In the current state of NLTE modeling, the radial magnetic field gradient in HD 58260 is real and it cannot be ascribed to an incorrect limb-brightening.

No conclusion concerning the decrease in field strength with altitude is possible unless new observations of the Stokes Q and U profiles provide us with the transverse component of the magnetic field (Leone et al. 2017). At this stage,

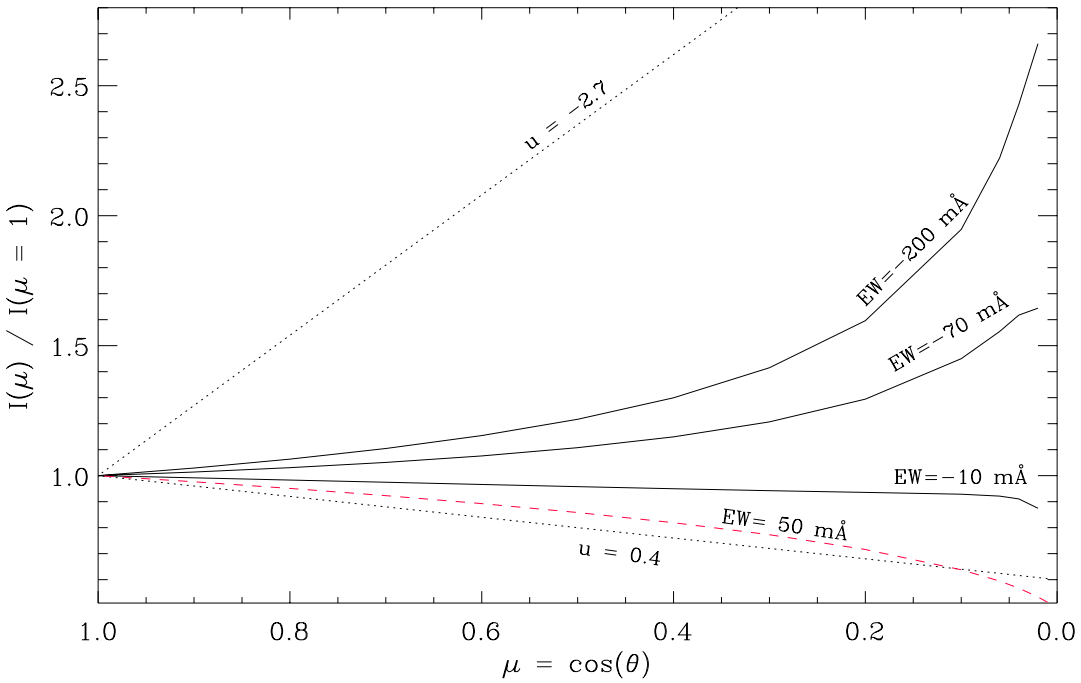

Figure 4. SYNSPEC5.1 intensity, across the stellar disk, of the FeII 7513.176 Å spectral line in emission (negative Equivalent Widths, EW) for different abundance values. θ is the angle between LoS and the direction of the emerging flux. For comparison, the intensity variation of the LTE line in absorption (EW = 50 mÅ; red-dashed) is reported together with (dotted) linear ($u = 0.4$) limb-darkening and ($u = -2.7$) limb-brightnening.

it is not possible to foresee the consequence of a more compact magnetosphere on the synchrotron and auroral radio emission (Leto et al. 2021) from this class of stars.

The estimated scale of the vertical gradient of the magnetic field of HD 58260 is $\sim 0.1\,\mathrm{G\,km^{-1}}$. The Sun is the only other astrophysical place where the vertical gradient of the magnetic field has been observed: 1 - 4 $\mathrm{G\,km^{-1}}$ in solar spots (Joshi et al. 2017) and $10^{-4}\,\mathrm{G\,km^{-1}}$ in the corona (Gelfreikh et al. 1997). Indeed the resemblance between HD 58260 and the Sun could go further. Tan et al. (2020) have shown that the magnetic-gradient pumping mechanism can power energetic particle up-flows that are responsible for solar eruptions. These authors have also shown that the condition for magnetic-gradient pumping is the possibility for a charged particle to make at least a complete circle around magnetic lines before a collision with other particles. In practise, the gyro-frequency has to be larger than collision rate: $\nu_g > \nu_c$. The very presence of lines in emission is proof of an electron collision rate smaller than Einstein spontaneous-emission probability (A_{ji}, for transition $j \rightarrow i$), so that magnetic-gradient pumping is certainly at work in the case $\nu_g > A_{ji} > \nu_c$, with $A_{ji} \approx 10^7\,\mathrm{s^{-1}}$ for lines listed in Table 2. As to electrons, the non-relativistic gyro-frequency ν_g^e ($= 2.8\,\mathrm{MHz\,G^{-1}}$) is equal to 16.8 GHz at the magnetic pole, that is $\nu_g^e \approx 10^3 A_{ji}$. In a completely ionized plasma, proton collision rate is 60 times smaller than electron one and this leads to $\nu_g^p \approx 17 A_{ji}$. It appears that not only protons but also many light ions can be subject to the magnetic-gradient pumping mechanism in an early B-type star like HD 58260. The less demanding case $A_{ji} > \nu_g > \nu_c$ is more difficult to be evaluated.

HD58260 presents UV spectral lines in emission (Shore & Brown 1990) that are an unquestionable evidence of a high-temperature plasma wrapping the star. However, as already known from Pedersen (1979), we found no H_α emission in the here analyzed ESPaDOnS spectra (according to Shultz et al. (2019a)), neither X-ray emission has been reported by Petit et al. (2013) or radio emission by Linsky et al. (1992); Kurapati et al. (2017). A behaviour different than other similar stars that can present some or even all these phenomena, like σ Ori E showing X-ray emission (Sanz-Forcada et al. 2004), UV lines (Shore & Brown 1990), H_α emission (Pedersen 1979) and radio emission (Cassinelli 1985). If such a pumping mechanism is indeed at work in magnetic stars with high-energy emission phenomena (e.g. X-ray, UV spectral lines of highly ionized species, H_α (Leone et al. 2010) and radio), many unsolved problem can be addressed. The extra flow of energetic particles and a magnetic gradient different than for a dipole one could explain

why magnetospheres are not ubiquitous. Magnetospheres would be the result of the interplay of 1) accelerated charges able, at short stellar distances, to ionize at least up to Si III (33.5 eV) and C III (47.9 eV), and at large distances to contribute to the filling of the H_α (< 13.6 eV) emitting torus; and 2) field gradient, changing the location of the H_α emitting torus or even preventing its existence, as well the position of the centrifugal breakout (Havnes & Goertz 1984). Pumping could also play a role in the stellar wind mass-loss rates necessary to explain the observed radio emission from rotating magnetospheres. These 10^{-10} - $10^{-9} M_\odot yr^{-1}$ rates (see Leto et al. 2020, for a complete list of references) are much larger than predicted for main sequence B-type stars (Krtička 2014) or observed ($< 10^{-12} M_\odot yr^{-1}$) in the UV spectrum of the radio source CU Vir (Krtička et al. 2019).

ACKNOWLEDGMENTS

We acknowledge financial contribution from the agreement ASI-INAF n.2018-16-HH.0.

REFERENCES

Alecian, G., & Stift, M. J. 2019, MNRAS, 482, 4519, doi: 10.1093/mnras/sty3003

Alexeeva, S., Ryabchikova, T., Mashonkina, L., & Hu, S. 2018, ApJ, 866, 153, doi: 10.3847/1538-4357/aae1a8

Alexeeva, S., Sadakane, K., Nishimura, M., Du, J., & Hu, S. 2019, ApJ, 884, 150, doi: 10.3847/1538-4357/ab41fa

Alexeeva, S. A., Ryabchikova, T. A., & Mashonkina, L. I. 2016, MNRAS, 462, 1123, doi: 10.1093/mnras/stw1635

Babcock, H. W. 1949, The Observatory, 69, 191

Bohlender, D. A., Brown, D. N., Landstreet, J. D., & Thompson, I. B. 1987, ApJ, 323, 325, doi: 10.1086/165830

Cassinelli, J. P. 1985, in NASA Conference Publication, Vol. 2358, NASA Conference Publication, 2–23

Catanzaro, G., Giarrusso, M., Leone, F., et al. 2016, MNRAS, 460, 1999, doi: 10.1093/mnras/stw923

Catanzaro, G., Giarrusso, M., Munari, M., & Leone, F. 2020, MNRAS, 499, 3720, doi: 10.1093/mnras/staa3108

Donati, J.-F., Catala, C., Landstreet, J. D., & Petit, P. 2006, in Astronomical Society of the Pacific Conference Series, Vol. 358, Astronomical Society of the Pacific Conference Series, ed. R. Casini & B. W. Lites, 362

Donati, J. F., Semel, M., Carter, B. D., Rees, D. E., & Collier Cameron, A. 1997, MNRAS, 291, 658, doi: 10.1093/mnras/291.4.658

Donati, J. F., Semel, M., & Rees, D. E. 1992, A&A, 265, 669

Garrison, R. F., Hiltner, W. A., & Schild, R. E. 1977, ApJS, 35, 111, doi: 10.1086/190468

Gelfreikh, G. B., Pilyeva, N. A., & Ryabov, B. I. 1997, SoPh, 170, 253, doi: 10.1023/A:1004967202294

Gray, D. F. 1992, The observation and analysis of stellar photospheres., Vol. 20 (Cambridge University Press)

Havnes, O., & Goertz, C. K. 1984, A&A, 138, 421

Hubbard, E. N., & Dearborn, D. S. P. 1982, ApJ, 254, 196, doi: 10.1086/159723

Järvinen, S. P., Hubrig, S., Ilyin, I., et al. 2018, A&A, 618, L2, doi: 10.1051/0004-6361/201833171

Joshi, J., Lagg, A., Hirzberger, J., Solanki, S. K., & Tiwari, S. K. 2017, A&A, 599, A35, doi: 10.1051/0004-6361/201527060

Krtička, J. 2014, A&A, 564, A70, doi: 10.1051/0004-6361/201321980

Krtička, J., Mikulášek, Z., Henry, G. W., et al. 2019, A&A, 625, A34, doi: 10.1051/0004-6361/201834937

Kudryavtsev, D. O., & Romanyuk, I. I. 2009, in Cosmic Magnetic Fields: From Planets, to Stars and Galaxies, ed. K. G. Strassmeier, A. G. Kosovichev, & J. E. Beckman, Vol. 259, 411–412, doi: 10.1017/S1743921309030919

Kurapati, S., Chandra, P., Wade, G., et al. 2017, MNRAS, 465, 2160, doi: 10.1093/mnras/stw2838

Landi Degl'Innocenti, E., & Landolfi, M., eds. 2004, Astrophysics and Space Science Library, Vol. 307, Polarization in Spectral Lines, doi: 10.1007/978-1-4020-2415-3

Lanz, T., & Hubeny, I. 2007, ApJS, 169, 83, doi: 10.1086/511270

Leone, F., Bohlender, D. A., Bolton, C. T., et al. 2010, MNRAS, 401, 2739, doi: 10.1111/j.1365-2966.2009.15858.x

Leone, F., Scalia, C., Gangi, M., et al. 2017, ApJ, 848, 107, doi: 10.3847/1538-4357/aa8d72

Leto, P., Trigilio, C., Buemi, C. S., et al. 2020, MNRAS, 499, L72, doi: 10.1093/mnrasl/slaa157

Leto, P., Trigilio, C., Krtička, J., et al. 2021, MNRAS, doi: 10.1093/mnras/stab2168

Linsky, J. L., Drake, S. A., & Bastian, T. S. 1992, ApJ, 393, 341, doi: 10.1086/171509

Mashonkina, L. 2020, MNRAS, 493, 6095, doi: 10.1093/mnras/staa653

Mashonkina, L., Ryabchikova, T., Alexeeva, S., Sitnova, T., & Zatsarinny, O. 2020, MNRAS, 499, 3706, doi: 10.1093/mnras/staa3099

Mathys, G. 1990, A&A, 232, 151

—. 1994, A&AS, 108

Mayor, M., Pepe, F., Queloz, D., et al. 2003, The Messenger, 114, 20

Mitskevich, A. S., & Tsymbal, V. V. 1992, A&A, 260, 303

Neiner, C., Henrichs, H. F., Floquet, M., et al. 2003, A&A, 411, 565, doi: 10.1051/0004-6361:20031342

Nesvacil, N., Hubrig, S., & Jehin, E. 2004, A&A, 422, L51, doi: 10.1051/0004-6361:20048001

Pedersen, H. 1979, A&AS, 35, 313

Petit, V., Owocki, S. P., Wade, G. A., et al. 2013, MNRAS, 429, 398, doi: 10.1093/mnras/sts344

Preston, G. W. 1969, ApJ, 158, 1081, doi: 10.1086/150266

Ramírez Vélez, J. C. 2020, MNRAS, 493, 1130, doi: 10.1093/mnras/staa301

Romanyuk, I., & Kudryavtsev, D. 2004, in The A-Star Puzzle, ed. J. Zverko, J. Ziznovsky, S. J. Adelman, & W. W. Weiss, Vol. 224, 602–604, doi: 10.1017/S1743921305009415

Sadakane, K., & Nishimura, M. 2017, Publications of the Astronomical Society of Japan, 69, doi: 10.1093/pasj/psx024

Sanz-Forcada, J., Franciosini, E., & Pallavicini, R. 2004, A&A, 421, 715, doi: 10.1051/0004-6361:20047159

Scalia, C., Leone, F., Gangi, M., Giarrusso, M., & Stift, M. J. 2017, MNRAS, 472, 3554, doi: 10.1093/mnras/stx2090

Shore, S. N., & Brown, D. N. 1990, ApJ, 365, 665, doi: 10.1086/169520

Shultz, M. E., Wade, G. A., Rivinius, T., et al. 2018, MNRAS, 475, 5144, doi: 10.1093/mnras/sty103

—. 2019a, MNRAS, 490, 274, doi: 10.1093/mnras/stz2551

—. 2019b, MNRAS, 485, 1508, doi: 10.1093/mnras/stz416

Sigut, T. A. A., Landstreet, J. D., & Shorlin, S. L. S. 2000, ApJL, 530, L89, doi: 10.1086/312499

Tan, B.-L., Yan, Y., Li, T., Zhang, Y., & Chen, X.-Y. 2020, Research in Astronomy and Astrophysics, 20, 090, doi: 10.1088/1674-4527/20/6/90

Wade, G. A., Maíz Apellániz, J., Martins, F., et al. 2012, MNRAS, 425, 1278, doi: 10.1111/j.1365-2966.2012.21523.x

Wade, G. A., Neiner, C., Alecian, E., et al. 2016, MNRAS, 456, 2, doi: 10.1093/mnras/stv2568

Wahlgren, G. M., & Hubrig, S. 2004, A&A, 418, 1073, doi: 10.1051/0004-6361:20034257

Wolff, S. C. 1978, PASP, 90, 412, doi: 10.1086/130349